

Cavity Beam Position Monitor for the ILC Main Linac: Status and Plans

Laura Karina Pedraza^{1,2,*}, Nuria Fuster Martínez^{1,3}, Daniel Esperante Pereira^{1,2}, Benito Gimeno Martínez^{1,2}, Daniel González Iglesias^{1,2}, and César Blanch Gutiérrez^{1,3}

¹Instituto de Física Corpuscular (IFIC)

²Universidad de Valencia (UV)

³Consejo Superior de Investigaciones Científicas (CSIC)

Abstract. This work describes the preliminary study and evaluation of the design of a cavity beam position monitor (cBPM) for the Main Linac at the International Linear Collider (ILC) project. It is required to design and build a prototype to be tested together with a superconducting quadrupole in a cryostat, with a spatial resolution of less than 1 micron. The design of a re-entrant cBPM by CEA Saclay is used as the starting point for this analysis, where the geometry is evaluated to identify areas for improvement. A typical analog read-out system is simulated, allowing for a detailed evaluation of the impact of each component and providing opportunities to further estimate the device's performance. Finally, the numerical BIR-ME 3D method is employed to estimate the cBPM output.

1 Introduction

1.1 Motivation

For future particle colliders, cavity Beam Position Monitors (cBPMs) have emerged as the optimal solution for precisely measuring beam position, which is crucial for guiding and stabilizing high-energy beams with nanometer precision. This, in turn, enhances luminosity at the interaction point. For the ILC, achieving the design luminosity for particle physics experiments requires the preservation of low vertical emittance, ϵ_y , along the Main Linac. High-resolution BPMs are therefore essential, as it is considered necessary to attain spatial resolution on the order of nanometers. Due to their resonant behavior, cavity BPMs offer higher position sensitivity, allowing for greater resolution in determining the beam's position, which meets the ILC requirements [1].

1.2 Project definition

Development is underway for a cryostat that accommodates a reentrant cBPM and a superconducting quadrupole (SCQ) for the ILC Main Linac. Aligning the SCQ and cBPM centers within the cryostat is crucial for accurate beam position determination. Additionally,

*e-mail: Laura.Pedraza@ific.uv.es

the BPM prototype must be capable of measuring the beam position on a bunch-by-bunch basis, with temporal and spatial resolutions of less than 396 ns and 1 μm , respectively.

The model developed by CEA Saclay in collaboration with DESY, for a re-entrant cBPM used in the X-FEL, in reference [2], is currently under study. The aim is to improve the performance of the BPM through an evaluation of the design. Modifying the geometry could enhance sensitivity, as well as temporal and spatial resolution. Improving the read-out system could also increase spatial resolution.

The future cBPM and its associated electronics readout system will undergo testing at ATF under ambient conditions and subsequently, cryogenic temperature tests are foreseen with installation of the cryomodule at the end of the ATF linac.

2 The re-entrant cavity BPM

Resonant cBPMs operate based on the principle of measuring specific field configurations resonating at certain frequencies within a cavity. Short beam bunches can couple with the TM (transverse magnetic) modes of the cavity, where in a pill-box cavity, the *dipole* mode TM_{110} provides information on the transverse position of the beam. The *monopole* mode TM_{010} can be used as a reference for the measurement [3]. The dipole mode has two polarizations: one in the x -direction and another in the y -direction, allowing for measurements in two orthogonal directions.

2.1 Theory of the cBPM

This section describes briefly the theory of a pill-box cBPM, but the same principle applies for a re-entrant cBPM. For detailed explanation, refer to [4].

A Gaussian-distributed bunch with length σ_z and charge q can induce the TM modes of the pill-box, which will resonate inside the cavity and decay exponentially. According to the fundamental theorem of beam loading, the voltage of a resonant mode mnp , with angular frequency ω_{mnp} , excited by the beam, can be defined as

$$V_{b \rightarrow m} = \frac{\omega_{mnp}}{2} \left(\frac{R}{Q} \right)_{mnp} q \exp \left(-\frac{\omega_{mnp}^2 \sigma_z^2}{2c_0^2} \right) \quad (1)$$

which depends on the normalized shunt impedance $(R/Q)_{mnp}$ [5].

The energy stored in the cavity after passage of the beam can be derived from the definition of (R/Q) as

$$W_s = \frac{V_{b \rightarrow m}^2}{\omega_{mnp} (R/Q)_{mnp}} = \frac{\omega_{mnp}}{4} \left(\frac{R}{Q} \right)_{mnp} q^2 \exp \left(-\frac{\omega_{mnp}^2 \sigma_z^2}{c_0^2} \right) \quad (2)$$

The output power can then be obtained from the definition of the external quality factor Q_{ext}

$$P_{\text{out}} = \frac{\omega_{mnp} W_s}{Q_{\text{ext}}} = \frac{\omega_{mnp}^2 q^2}{4} \frac{1}{Q_{\text{ext}}} \left(\frac{R}{Q} \right)_{mnp} \exp \left(-\frac{\omega_{mnp}^2 \sigma_z^2}{c_0^2} \right) \quad (3)$$

And finally, the output voltage with impedance Z is defined as

$$V_{\text{out},0} = \sqrt{Z P_{\text{out}}} = \frac{\omega_{mnp} q}{2} \sqrt{\frac{Z}{Q_{\text{ext}}} \left(\frac{R}{Q} \right)_{mnp}} \exp \left(-\frac{\omega_{mnp}^2 \sigma_z^2}{2c_0^2} \right). \quad (4)$$

The normalized shunt impedance (R/Q)_{mnp} can be easily calculated by means of the expression of the electric fields of the modes, well-known for a pill-box cavity. For a beam with an offset δx , it can be shown that $[R/Q]_{110} \propto (\delta x)^2$ and $[R/Q]_{010} \sim \text{constant}$. It is then proven that

$$V_{\text{out},110} \propto \delta x \quad \text{and} \quad V_{\text{out},010} \sim \text{constant}.$$

In this way, detecting the *dipole* mode will provide information on the beam position δx . A *monopole* mode, from a reference cBPM can be used to normalize the dipole voltage, allowing for a measurement that is solely dependent on position (see Figure 1).

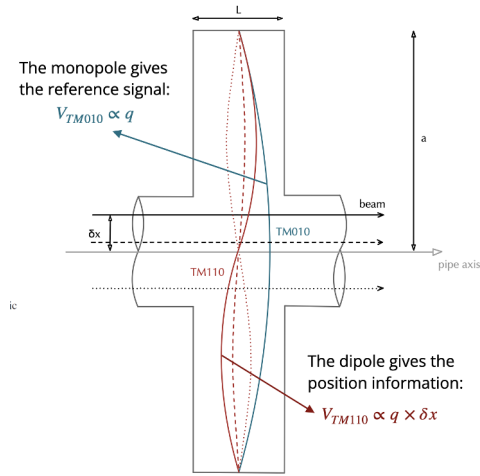


Figure 1: Schematic representation of the E-field induced for the monopole (blue) and dipole (red) in a cavity BPM [3].

Since the recovered signal out of the cavity oscillates with the frequency of the mode ω_{mnp} and decays exponentially, the time-dependent output will be

$$V_{\text{out}}(t) = V_{\text{out},0} \sin(\omega_{mnp}t + \varphi) \exp\left(-\frac{t}{\tau}\right) \quad (5)$$

where $\tau = 2Q_L/\omega_{mnp}$ defines the temporal resolution of the BPM and depends on the loaded quality factor Q_L that considers the total dissipation of power of the cavity. The trajectory angle and attack angle of the bunch can contribute to the output voltage. These angles cause a signal that is $\pi/2$ out of phase with the one induced by a beam parallel to the z -axis [6]. Therefore, both the amplitude and phase of the output signal must be detected to perform accurate measurements.

2.2 Existing model from CEA Saclay

A re-entrant cBPM is similar to a pill-box BPM but includes a coaxial cylinder attached to the cavity. The re-entrant cBPM model developed by CEA Saclay is shown in Figure 2. This BPM model is advantageous due to its mechanical simplicity and performance. It has been shown to achieve spatial resolution better than $10 \mu\text{m}$ for a dynamic range of $\pm 5 \text{ mm}$ and can perform bunch-to-bunch measurements at the X-FEL. Table 1, taken from [2], provides general information on the BPM radio-frequency (RF) characteristics. The resonance frequency and loaded quality factor provide an estimation of the temporal

Resonant mode	Frequency (GHz)	Q_L	R/Q @ 5 mm (Ω)	R/Q @ 10 mm (Ω)
Monopole	1.255	23.8	12.9	12.9
Dipole	1.724	59	0.27	1.15

Table 1: RF characteristics of the BPM model developed by CEA Saclay [2].

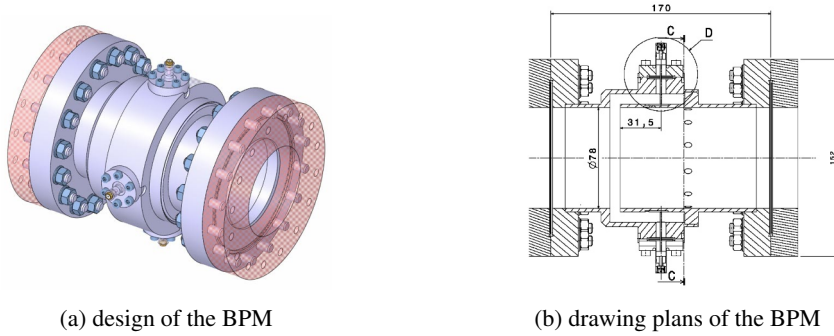


Figure 2: Re-entrant BPM model developed by CEA Saclay [2] [7].

resolution, $\tau = 10.9$ ns. It is important to note that this temporal resolution can, in practice, be larger since the analog read-out system can enlarge the signals. The normalized shunt impedance (R/Q) at a certain distance from the center of the pipe represents the sensitivity, as it contributes (among other factors) to the coefficient of δx . It is notable that the normalized shunt impedance is constant for the monopole mode and has a squared dependence on the transverse position inside the cavity, as predicted by theory.

3 Geometry studies on CST Studio Suite

The RF characteristics discussed in the previous section are primarily determined by the geometry of the cavity and the placement of the output ports. Slight modifications to some dimensions can enhance the BPM performance. Commercial software CST Studio Suite can be used to perform a 3D electromagnetic analysis of the cBPM [8].

The loaded quality factor is crucial because it determines the length of the output signals, according to the definition of the decay time τ . A higher Q_L will allow more information to be retrieved from $V_{out}(t)$ and could improve the spatial resolution of the cBPM. However, signals must decay fast enough (less than 369 ns) if bunch-to-bunch measurements are to be achieved. Additionally, increasing (R/Q) for the dipole mode will enhance sensitivity and, consequently, the spatial resolution. Since both reference and position signals are extracted from the same cBPM, it is advantageous to lower (R/Q) for the monopole mode, as this mode is excited with greater strength and is likely to overshadow the dipole mode signal.

These geometric modifications must always be made with certain restrictions and guidelines in mind. Mechanically, the device must fit properly when attached to the SCQ and the cryomodule. This will be further considered once the plans for the full cryostat are available.

Furthermore, it must be ensured that the cBPM does not exhibit significant *cross-talk*. This phenomenon occurs when the dipole mode polarizations are not completely isolated; thus, a beam with a purely horizontal offset can induce a non-zero reading in the vertical direction, and vice versa. This can be controlled by evaluating the coupling between ports through the scattering parameter S_{12} , where 1 and 2 represent any orthogonal ports.

3.1 Parametric studies

Using the *eigenmode* solver in CST, a parametric study was conducted to gain a preliminary understanding of the main dimensions that significantly impact the aforementioned RF characteristics, using as a starting point the design in reference [2].

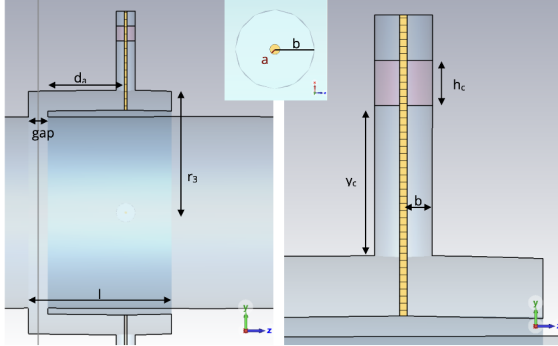


Figure 3: Dimensions considered for parametric study on Saclay's BPM.

It was observed that the length of the cavity l and the distance from the antenna to the gap d_a had a significant influence on Q_L . The height of the ceramic seal h_c and the radius of the inner conductor a at the output port also significantly impact Q_L , but it was later determined that these dimensions are usually standardized and should be fixed. Additionally, l also affects $(R/Q)_{\text{dipole}}$.

Further study is needed, as modifying a single dimension can simultaneously affect other RF characteristics. A cross-examination that also considers isolation between ports and the impact of wakefields is ongoing.

4 Simulation of the analog signal processing in MATLAB

In parallel with the geometry design studies, a simulation of the analog read-out chain was conducted using MATLAB. This study aimed to provide a closer understanding of the role of the main components in a classical read-out chain used for cBPMs. A detailed examination of this could potentially enable us to identify steps that could be modified to enhance the cBPM performance in terms of resolution.

4.1 Simulation approach

Initially, the CST *wakefield* solver allows for the simulation of the signal induced by a passing bunch on the four output ports of the cBPM. The bunch is simulated as a Gaussian bunch with charge $q = 3.2$ nC, length $\sigma_z = 5$ mm, and offset $\delta x = 500$ μm . The signal at the ports, as a function of time, can be retrieved by placing waveguide ports at the end of each output antenna.

Figure 4 features the scheme of the analog read-out chain that uses the cBPM signal to obtain the transverse position measurement. This analog signal processing inspired on electronics used by CEA Saclay for this BPM [2] and by down-converting electronics used for the Extreme Light Infrastructure (ELI) [9]. A 180° hybrid coupler combines signals from opposite ports to obtain the position signal, which contains information from the dipole mode. The normalizing signal comes from a reference cavity, whose monopole mode has the same oscillation frequency as the dipole mode of the signal cavity. The rest of the scheme involves simple down-conversion, where the position and reference signals are treated similarly. Lower-impact components, such as amplifiers and attenuators, will later be used

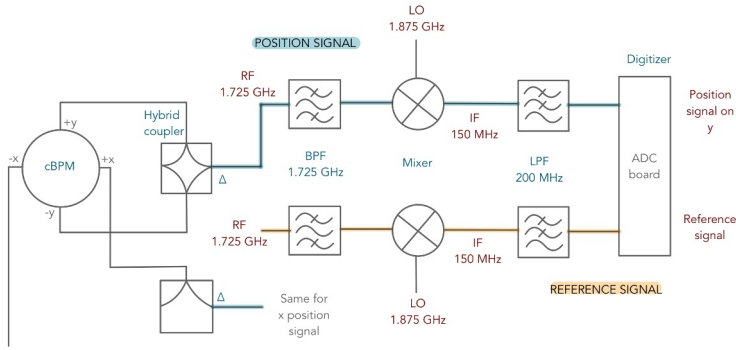
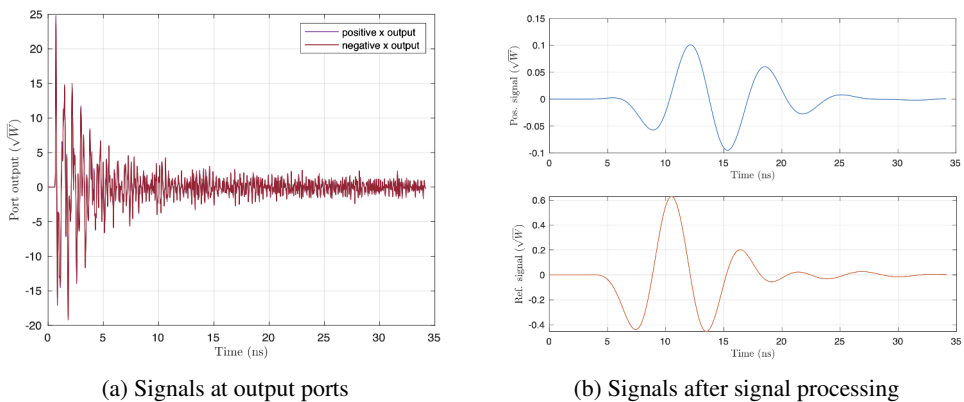


Figure 4: Scheme of analog read-out system simulated with MATLAB.

to control signal amplitudes and avoid saturation, but they are not included in the current simulation. The signals are then filtered with a BPM at the resonance frequency of the dipole mode: 1.725 GHz using a band-pass filter (BPF). Then, they are mixed with a local oscillator (LO) operating at 1.875 GHz to down-convert to 150 MHz. A low-pass filter (LPF) removes the up-converted term, and finally, the signals are digitized at a rate of 500 MS/s. All components are initially simulated as ideal to assess their influence on the signals in both the time and frequency domains. A more realistic simulation, including imperfections and losses, is underway. This will enable a proper estimation of the spatial and temporal resolution.

4.2 Simulation results with ideal read-out chain

Figure 5 shows the successful acquisition of position and reference signals, as well as the down-conversion process, which allows for the determination of the output signal characteristics needed for position measurements. It is noted that during this process, signals are slightly delayed and enlarged. After a step-by-step evaluation, it was concluded that this effect is primarily caused by the filters.



(a) Signals at output ports

(b) Signals after signal processing

Figure 5: Output cBPM signals before and after simulated read-out chain.

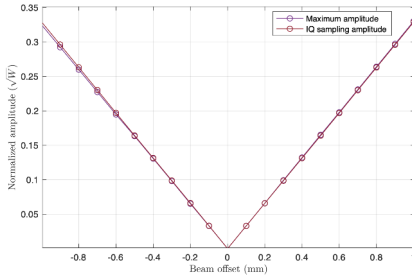


Figure 6: Normalized amplitude of output signal as a function of the beam position.

The amplitudes of the digitized position and reference signals were determined either by taking the maximum or using an IQ-demodulation method. Figure 6 shows the normalized amplitude of the output signal for various beam positions, where the linearity predicted by theory in Section 2 was observed. A non-ideal simulation will allow for the examination of other performance features, such as resolution and dynamic range.

5 BIR-ME 3D method on a cBPM

An alternative approach for estimating the cBPM output signals at the ports is the BIR-ME (Boundary Integral Resonant - Mode Expansion) 3D method [10].

5.1 Method overview and implementation

This is a hybrid technique that uses CST field results for an empty, closed resonant cavity and allows for the evaluation of the RF power extracted at the output ports when the cavity is excited by a beam. For a given operating frequency, the numerical method can calculate the power consumed by the cavity and delivered to the ports, the amplitude and phase of the output RF signal, as well as the external and loaded quality factors, among other parameters.

The CST *eigenmode* solver provides the 3D electromagnetic field results for a closed cavity, which can be exported and used as input for the BIR-ME method. The technique is capable of computing the coupling between the beam, the closed cavity and the output waveguide ports. In this case, the output ports are coaxial waveguides; thus, the intensity generated by the beam for a mode m leading to port (i) is calculated as

$$I_b^{(i)} = \sum_{m=1}^3 \frac{\kappa_m}{k^2 - \kappa_m^2} \int_{S^{(i)}} \vec{H}_m \cdot \vec{h}_{TEM}^{(i)} dS \int_V \vec{E}_m \cdot \vec{J}_b dV \quad (6)$$

where $k = 2\pi f/c_0$ (and f is the operation frequency), κ_m allows to consider the Ohmic losses of the modes as

$$\kappa_m \simeq k_m \left(1 - \frac{1}{2Q_m}\right) + j \frac{k_m}{2Q_m}$$

where $k_m = 2\pi f_m/c_0$ (f_m is the resonance frequency of mode m), H_m and E_m are respectively the magnetic and electric fields of mode m , $h_{TEM}^{(i)}$ is the magnetic field of the TEM mode on the coaxial waveguide port (i), and J_b is the Fourier Transform of \mathfrak{J}_b the beam current density, defined initially for punctual charges, as

$$\vec{\mathfrak{J}}_b = \sum_{n=1}^N q_n \delta(\vec{r} - \vec{r}_n) \vec{v}_n$$

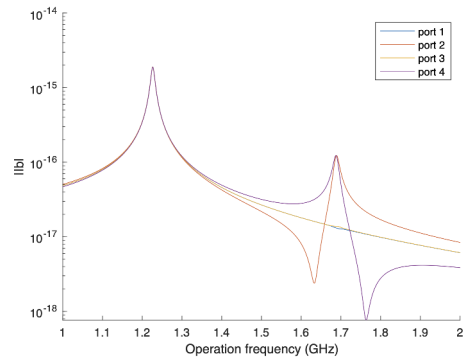
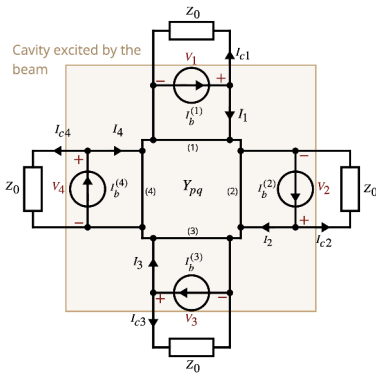
where q_n , v_n and r_n are the charge, speed and position of a punctual charge n [10].

It is convenient to note that equation 6 considers the contribution of 3 modes m : the monopole mode (TM₀₁₀) and the two polarization of the dipole mode (TM₁₁₀). Moreover,

the calculation of $I_b^{(i)}$ involves two integrals representing different couplings. The volume integral accounts for the coupling between the cavity and the beam, while the surface integral represents the coupling between the cavity and the output ports.

5.2 Simulation of the cBPM output signal

The BIR-ME method employs the scheme on figure 7a as the equivalent for the cBPM. The cavity excited by the beam is represented by the underlined part of the diagram, where there are four voltage sources and their corresponding intensity $I_b^{(i)}$. It also considers the admittance matrix of the closed cBPM Y_{pq} and the four extremities represent each one of the output ports where (1) and (3) are the vertical ones and (2) and (4) are the horizontal ones.



(a) Schematic representation of the cBPM on BIR-ME

(b) $|I_b^{(i)}$ as a function of frequency for $\delta x = 5$ mm

Figure 7: BIR-ME 3D cBPM simulation and results.

The simulation was performed for a beam with a horizontal offset as shown in Figure 7b. The results are consistent with the wakefield simulation performed by CST, where a high resonance is observed at the frequency of the monopole mode (1.25 GHz) and a smaller resonance at the frequency of the dipole mode (1.72 GHz), which is only present on the horizontal ports.

This new implementation of the method for these devices is highly beneficial as it provides new insights into the cBPM performance. Unlike CST, it allows for an unrestricted definition of the beam. Further application of this method will offer new estimations of the output voltage and RF characteristics of the BPM.

6 Conclusion

The resonant BPM developed by CEA Saclay [2] enables bunch-to-bunch measurements at the ILC with a resolution on the order of micrometers. Various evaluation methods are being employed to enhance spatial resolution to meet the Main Linac requirements. The CEA Saclay design is under evaluation to improve BPM sensitivity and spatial resolution. Simulation of the read-out system in MATLAB allows for the assessment of the influence of all components on the overall system performance. Additionally, a novel numerical approach, BIR-ME 3D, which estimates the cBPM output signal, is currently being implemented and

will be compared with results from CST Studio Suite. Lastly, a preliminary plan is underway to develop a prototype that integrates the SCQ and BPM assembly into a test cryostat.

References

- [1] Ronald Lorenz. Cavity Beam Position Monitors. In: AIP Conference Proceedings (1998).
- [2] Claire Simon, et al. Performance of a reentrant cavity beam position monitor. *Physical Review Special Topics - Accelerators and Beams* 11.8 (2008)
- [3] Michele Viti, Resonant Cavities as Beam Position Monitor. Deutsches Elektronen-Synchrotron DESY (2009).
- [4] Laura Pedraza, Cavity Beam Position Monitors State of the Art and Design Studies in the Context of the ILC Project. Student Paper LTH Lund University (2023).
- [5] T. Nakamura, Master Thesis: Development of BPM with high position resolution. University of Tokyo (2008).
- [6] Walston, Sean, et al., Performance of a high resolution cavity beam position monitor system. *Nuclear Instruments and Methods in Physics Research Section A: Accelerators, Spectrometers, Detectors and Associated Equipment* (2007).
- [7] Claire Simon, et al. Beam position monitors using a reentrant cavity. *Proceedings of DIPAC* (2007).
- [8] Software de Simulación Y Análisis de EM 3D CST Studio Suite. www.3ds.com, www.3ds.com/es/productos-y-servicios/simulia/productos/cst-studio-suite/. Accessed 6 Sept (2024).
- [9] Oran Friar and Alexey Lyapin, Building, Optimizing and Measuring the Performance of Downconverting Electronics Using X-Microwave Modules. PH4100 Major Project Report RHUL (2022).
- [10] Benito Gimeno and RADES collaboration, Wide-band full-wave electromagnetic modal analysis of the coupling between dark-matter axions and microwave resonators, AITANA Seminar (2024).